hydrology

MDPI

Article

Flood Exposure Dynamics and Quantitative Evaluation of Low-Cost Flood Control Measures in the Bengawan Solo River Basin of Indonesia

Badri Bhakta Shrestha *, Mohamed Rasmy and Daisuke Kuribayashi

International Centre for Water Hazard and Risk Management (ICHARM), Public Works Research Institute (PWRI), Tsukuba 305-8516, Ibaraki, Japan; abdul@pwri.go.jp (M.R.); kuribayashi-d673cm@pwri.go.jp (D.K.)
* Correspondence: babhash@gmail.com; Tel.: +81-29-879-6815

Abstract: The frequent occurrence of floods puts additional pressure on people to change their activities and alter land use practices, consequently making exposed lands more vulnerable to floods. It is thus crucial to investigate dynamic changes in flood exposures and conduct quantitative evaluations of flood risk-reduction strategies to minimize damage to exposed items. This study quantitatively assessed dynamics of flood exposure and flood risk, and evaluated the effectiveness of flood control measures in the Bengawan Solo River basin, Indonesia. The Water and Energy Budget-Based Rainfall–Runoff–Inundation Model was employed for flood simulation for different return periods, and then dynamics of flood exposures and flood risk were assessed. After that, the effectiveness of flood control measures was quantitively evaluated. The results show that settlement/built-up areas and population are increasing in flood-prone areas. The flood-exposed paddy field and settlement areas for 100-year flood were estimated to be more than 950 and 212.58 km^2, respectively. The results also show that the dam operation for flood control in the study area reduces the flood damage to buildings, contents, and agriculture by approximately 21.2%, 20.9%, and 25.1%, respectively. The river channel improvements were also found effective to reduce flood damage in the study area. The flood damage can be reduced by more than 60% by implementing a combination of a flood control dam and river channel improvements. The findings can be useful for planning and implementing effective flood risk reduction measures.

Keywords: exposures; land use and land cover; flood damage; river channel improvement; dam

Academic Editor: Aristoteles Tegos

Received: 17 January 2025
Revised: 10 February 2025
Accepted: 15 February 2025
Published: 17 February 2025

Citation: Shrestha, B.B.; Rasmy, M.; Kuribayashi, D. Flood Exposure Dynamics and Quantitative Evaluation of Low-Cost Flood Control Measures in the Bengawan Solo River Basin of Indonesia. *Hydrology* **2025**, *12*, 38. https://doi.org/10.3390/hydrology12020038

1. Introduction

A growing population and increasing development activities often put pressure on land systems, increasing environmental risks [1,2]. Changes in the land system in flood-prone areas may expose the areas to even higher environmental risks. It is thus crucial to understand the dynamics of flood exposure and corresponding flood-risk levels to reduce environmental risks and provide useful information for informed decision-making in practical environmental risk management and future land use planning [1].

The analysis of flood exposure changes, such as land use and land cover (LULC) changes or population changes, is essential to gain a better understanding of environmental issues [3], and it can provide more information for effective land use planning and management and environmental risk reduction [4]. The dynamics of land cover changes can be monitored and observed using historical land cover maps or remotely sensed satellite-based

images [5,6]. Numerous studies have focused on the analysis of LULC changes in different parts of the world [1,2,7–23]. Land cover maps created in past years and their changes can be the key information to understand the dynamics of flood exposures in flood-prone areas. In addition to the changes in land cover, demographic changes and spatial distributions also play an important role in flood risk assessment and planning adaptation measures. Flooding can have severe impacts on humans, and it is thus important to understand how exposed people in flood-prone areas are changing spatially and temporally in order to define their vulnerability and improve adaptation measures by identifying current and future risks [24]. Recent studies reported continuous increases in human exposure to floods due to changes in the hydrological system and land use [25–27]. The increasing rate of human exposure to floods might be higher in the future due to the combination of social and climate changes unless proper mitigation measures are taken. Spatiotemporal quantification of exposed people in flood-prone areas can be useful to improve emergency preparedness, evacuation, and human-risk reduction.

Floods often threaten the environment of exposed lands in rural and urban flood-prone areas, resulting in huge economic losses and disaster damage. The negative impact of floods can be reduced through non-structural and structural approaches, and more effectively by combining both approaches [28]. However, the efficient implementation of preventive measures requires the quantitative assessment of flood risk. One of the most important and informative non-structural approaches to reduce losses and prevent damage from floods is mapping flood hazards and risks [28]. Structural approaches to preventing floods include river channel improvements (e.g., channel deepening and widening, and levee construction), flood diversions, and flood-detention dams. The construction of new structural measures, such as flood storage dams, is challenging, particularly in developing countries, because of financial, political, and social issues. As Kawasaki et al. [29] pointed out, the construction of embankments would not be easy in some areas because it may require a large investment not only for constructing embankments but also for resettling people living on riverbanks. To address these issues, it is thus crucial to understand how existing river structures, such as dams and reservoirs, can be effectively used for flood control as low-cost flood control measures. In this study, low-cost flood control measures refer to flood control measures that can be implemented with a relatively low construction cost compared to large-scale structural measures, like building new flood control dams or levees. In addition, it is also crucial to understand the effectiveness of river channel improvements, such as channel deepening and widening, for reducing flood disasters. Channel widening and deepening can also be considered a relatively low-cost flood control method compared to other large-scale structural measures, such as construction of new flood control dams. Figure 1 shows the example of channel-dredging and -widening activities in the Pampanga River basin of the Philippines. Moreover, combining a flood control dam with river channel-improvement works is considered the most effective approach to significantly reduce flood damage. For example, in Japan, flood control has been dependent primarily on the construction of dams in the upper reaches of rivers to reduce flood peaks and on the construction of levees and floodways and channel dredging and widening in the lower reaches to safely and quickly discharge floodwaters [30].

This study focused on the quantitative analysis of spatiotemporal changes in the distributions of land cover areas and population exposed to flood risk, and it also aimed to evaluate the effectiveness of flood control measures for reducing disaster damage. The analyses were conducted using hydrologic–hydraulic model outputs in a flood loss estimation model. This study selected the Bengawan Solo River Basin (BSRB) as the study basin. First, Rainfall–Runoff–Inundation processes, using a hydrological–hydraulic model, were simulated for flood events of different return periods, and flood hazards in the basin

were analyzed. Then, dynamic changes in land cover and population using historical data were analyzed, and land cover areas or population exposed to flooding in the cases of flood events of different return periods were also assessed. Finally, to evaluate the effectiveness of flood control measures, flood hazards and damage were assessed for flood events of different return periods with and without flood control measures. The effectiveness of flood control measures for reducing damage was evaluated, focusing on the household and agriculture sectors.

Figure 1. Example of river channel-improvement activities in the Pampanga River basin of the Philippines. (Photos: Mr. Hilton Hernando, Pampanga River Basin Flood Forecasting and Warning Centre).

2. Materials and Research Methods

2.1. Study Area

The BSRB is the longest river on the island of Java in Indonesia, with a basin area of 15,839 km^2. Figure 2a shows the location of the BSRB and the study-area boundary with a topographical distribution. The average annual precipitation in the basin is approximately 2100 mm. The Wonogiri multipurpose dam with a reservoir capacity of 730 $\times$ 10^6 m^3 is located in the upper part of the basin. The purposes of the Wonogiri dam are flood control (flood storage capacity: 220 $\times$ 10^6 m^3), irrigation, raw water supply, and hydropower generation. The upper catchment area of the dam is 1350 km^2. The wet season usually lasts from November to April, and floods typically occur between December and March. Floods continue to be the most severe annual weather-related disaster in the basin, particularly in the lower part of the basin.

Figure 2b shows the spatial distribution of soil types in the study area based on the FAO/UNESCO soil map. Vertisols, which are rich in clay, are the most widespread soil type in the study area. Vertisols are the best soils for irrigated agricultural cultivation. Fluvisols were found in the lowland area of farthest downstream of the Solo River and also in the upstream part of the Madiun River. Both Vertisols and Fluvisols, which are naturally good fertile soils, can be considered good for agricultural cultivation. Other soil types found in the study area are Gleysols, Lithosols, Luvisols, Regosols, and Andosols.

2.2. Methodology

This study primarily consisted of three components: (i) flood hazard and risk analysis; (ii) analysis of social changes, such as land use and land cover, population changes, and the assessment of the dynamics of flood exposure; and (iii) flood damage assessment and the evaluation of the effectiveness of flood control measures (e.g., use of existing structures for flood control or river channel improvements) for reducing flood damage. The methods are described in detail in the following subsections.

2.2.1. Flood Hazard Analysis

For flood hazard and inundation analysis, this study employed the Water and Energy Budget-Based Rainfall–Runoff–Inundation (WEB-RRI) model, a hydrologic–hydraulic model, developed by Rasmy et al. [31]. The WEB-RRI model, which connects interactions

between surface flow and river flow, groundwater flow and soil moisture contents, and groundwater flow and river discharge, consists four components: (i) the Simple Biosphere Model 2 (SiB2) module for the vertical energy and water flux transfer between land and atmosphere, (ii) the vertical soil moisture distribution module for groundwater recharge, (iii) the 2-D diffusive wave lateral flow module for surface flow and groundwater flow, and (iv) the 1-D diffusive wave river flow module for river flow calculation [31]. The details on the WEB-RRI model and required input data and their sources can be found in Rasmy et al. [31]. This study applied calibrated and validated WEB-RRI model parameters used for the same basin by Shrestha et al. [32]. The details about model calibration and validation can be found in Shrestha et al. [32].

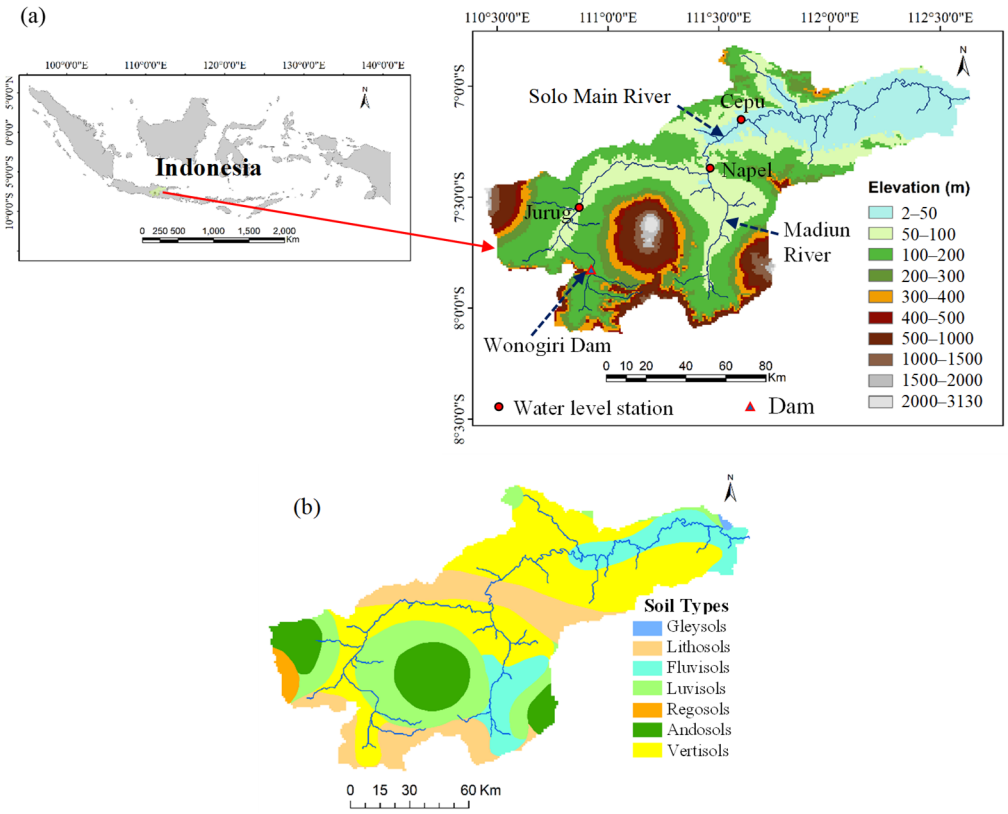

Figure 2. (**a**) Location of the Bengawan Solo River Basin (BSRB) and elevation distribution based on HydroSHEDS digital elevation model (https://www.hydrosheds.org/products/hydrosheds, accessed on 10 December 2023) and (**b**) soil types in the study area based on digital soil map of FAO/UNESCO (https://data.apps.fao.org/, accessed on 21 July 2022).

Previous researchers often used 500 m or 1000 m or larger grid sizes in the hydrologic–hydraulic model simulation such as in Rainfall–Runoff–Inundation (RRI) model or WEB-RRI model simulation for basin-level or areas with a larger catchment size, depending on the catchment size for efficient computation [28,31–37]. In this study, the WEB-RRI model was simulated for the entire river basin, and appropriate grid size, approximately 920 m (30-arc second), was used for the study area by referring to previous studies and considering the catchment area. The digital elevation model, flow direction, and flow accumulation, which were downloaded from the HydroSHEDS (https://www.hydrosheds.org/, accessed on 10 December 2023) at 30-arc second resolution, were used in the flood simulation model as topographical feature inputs. The soil-type distribution and related soil-water parameters (e.g., saturated hydraulic conductivity, saturated and residual social moisture contents, and Van Genutchen parameters) were obtained from the Food and Agriculture Organization (FAO) (https://www.fao.org/home/en/, accessed on 5 July 2023). Other forcing

inputs, such as air temperature, surface pressure, wind speed, radiation, and specific humidity, were obtained from the Japan Meteorological Agency's Japanese 55-year ReAnalysis (JRA-55) (https://jra.kishou.go.jp/JRA-55/index_en.html, accessed on 15 May 2024).

The river channel locations and network were determined using the flow accumulation and flow direction data downloaded from the HydroSHEDS. The resulting river network in the study area was found to be reasonably consistent with the actual river network. In the WEB-RRI model, the flow direction varies depending on local hydraulic gradients, and flow direction and flow accumulation data were used to determine only river channel locations and not for flood routing. The river cross-section was approximated as rectangular channel, and the river channel width and depth at each river cell corresponding to bankfull discharge were approximately calculated using empirical equations (Equations (1) and (2)) [33].

$$width = C_w \, A^{S_w} \tag{1}$$

$$depth = C_d \, A^{S_d} \tag{2}$$

where A is the upstream contributing catchment area in km^2, C_w (=5.5) and S_w (=0.3) are the empirical parameters of width, and C_d (=0.9) and S_d (=0.22) are the empirical parameters of depth. The units of width and depth are meters. Firstly, the default values of the parameters of these empirical relationships included in the RRI model were used, which were determined using the data of the river basins in the Southeast Asian countries [33], and these values were then adjusted or fine-tuned for the study area during the process of calibration and validation and also based on Google Earth images.

Flood hazard or inundation maps, which usually show the flood extent and depth caused by a flood of a target scale, are essential to implement practical land use management and flood preventive measures. The target scale for flood hazard analysis is generally decided based on the socio-economic conditions of the target area and the purpose of research. In practice, the scale of the recorded largest flood in the past or the scale of a 50- or 100-year flood is used as the target scale. To understand the flood characteristics of low-scale and extreme floods, this study simulated unsteady-state inundation during flood events of different return periods, i.e., 5, 10, 25, 50, 100, 150, and 200 years, using the calibrated and validated WEB-RRI model. Kudo et al. [34] found that the 4-day accumulated rainfall was strongly correlated with peak discharge for the BSRB, and they used 4-day annual maximum rainfall in the frequency analysis. Iwami et al. [35] also used 4-day rainfall for frequency analysis for the same study basin. By referring to previous studies, flood frequency analysis was thus conducted using the basin average (area average) 4-day annual maximum rainfall (i.e., annual maximum of total rainfall accumulated over a 4-day period) for the period from 1976 to 2009, based on the Gumbel distribution. The worst flood events in history are often used to design rainfall for specific return period in assessing flood hazards and damages because these events can help to estimate the potential extent of extreme flood scenarios, which can help with disaster planning and resource allocation [29,36–38]. Therefore, the spatial and temporal rainfall patterns of December 2007–January 2008, which led to a worst flood event, were selected to determine rainfall for flood events of different return periods. The rainfall intensity for each return period was obtained from frequency analysis. The rainfall hyetograph for a specific return period was estimated by multiplying the selected rainfall pattern of the 2007/2008 flood event by a conversion factor. The conversion factor for each return period was calculated as the ratio of the corresponding rainfall of the return period and the rainfall volume of the selected 2007/2008 rainfall pattern [28]. Then, flood simulations were performed using the WEB-RRI model by applying determined rainfall for a flood of a specific return period. The initial setting of the time step for surface flow, groundwater flow, and river

flow calculations was 600 s; however, the adaptive Runge–Kutta algorithm was applied in the model calculations, which may shorten the calculation time step if necessary [31].

ArcGIS 10.8, a geographic information system (GIS), was used to prepare a flood hazard or inundation map by overlaying or classifying inundation depth. The calculated flood inundation results from the model simulation were imported into ArcGIS, and then spatial analysis tools in ArcGIS were used to classify the areas based on flood depth. The flood inundation probability map was also prepared using ArcGIS by overlaying flood inundated areas calculated for different return periods (i.e., 5-, 10-, 25-, 50-, 100-, 150-, and 200-year flood) (overlaying inundated areas for lower return periods on top of those for higher return periods).

2.2.2. Social Changes and Exposure Assessment

This study analyzed changes in land cover and land use in the study basin using land cover maps in 1990, 2006, and 2020 and changes in population using the WorldPop population in 2000, 2010, and 2020 (Figure 3). Land cover maps of the study area were collected from the Ministry of Environment and Forestry, Indonesia, and the population data were downloaded from the WorldPop database (https://www.worldpop.org/, accessed on 25 June 2024).

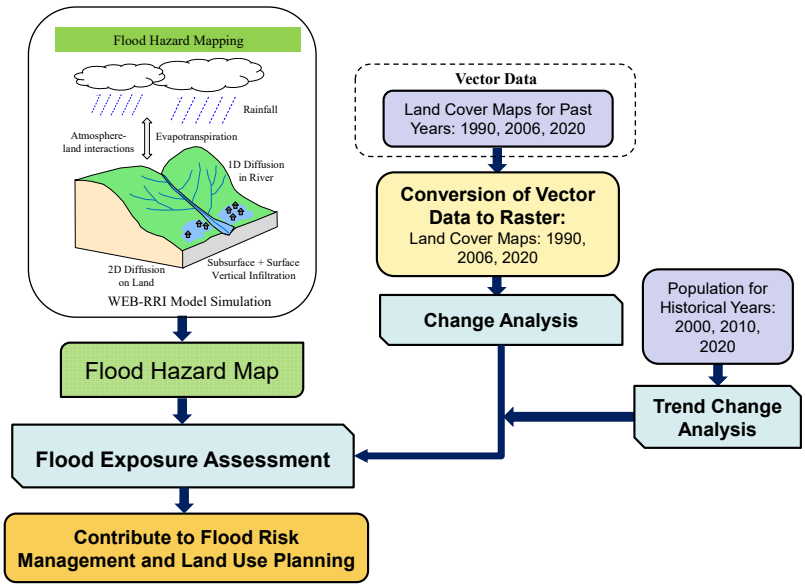

Figure 3. Overview of flood exposure assessment.

This study assessed social flood exposure, focusing on land cover areas and population, considering changes in land cover, land use, and population. By overlaying the land cover maps or population data with delineated flood hazard maps of different flood scales in a GIS, this study estimated exposed areas of each land cover class in flooding or exposed population in the flood-prone areas. To estimate exposed land cover areas or population in the flood-prone areas, first the generated raster layer of flood inundation depth from flood simulation for each return period flood was imported into ArcGIS, and then other relevant data, such as land cover or population data, were overlayed with imported flood inundation layer. Finally, the exposed land cover areas or population in the flood inundation areas were extracted using spatial analysis tools in ArcGIS.

2.2.3. Assessment of Flood Risk and Evaluation of Effectiveness of Low-Cost Flood Control Measures

This study evaluated the effectiveness of low-cost flood control measures such as use of the existing dam for flood control, focusing on flood damage to residential houses and rice crops. The channel widening and deepening can also be considered as a relatively low-cost flood control measure compared to other hard engineering options like building large levees or building new flood control dams or constructing extensive flood relief channels, as it primarily involves modifying the existing river channel without significant infrastructure additions; however, the cost can vary depending on the scale of the project, the topographical and geological characteristics, and the environmental factors. Thus, this study also considered quantitative evaluation of river channel-improvement works, such as channel widening and deepening for reducing the damage and risk.

To quantify damage with or without flood control measures, this study employed a damage estimation method and flood damage curves presented in Shrestha et al. [32] for houses and contents and those in Shrestha et al. [39] for rice crops. The total number of houses at each calculation grid was estimated based on the population at the grid and the average family size (3.7 people). The majority of the houses in the study area are masonry-walled (approximately 79%) and wooden-walled (approximately 21%) [32]. The average rebuilding value of a house was approximately IDR 106.64 million for masonry-walled house and IDR 90 million for wooden-walled house. The average exposure value of household contents (replacement value) per household was IDR 32.37 million [32]. Flood damage to houses and contents was defined as function of flood depth, while flood damage to rice crops was defined as function of both flood depth and duration. The growth stage of rice crops was considered the same as during the largest recorded flood event in 2007/2008. The volume and value of rice-crop loss were estimated using the following values referring to previous research [39]: a rice yield of 5230 kg/ha, a farm gate price of rice of 4650 IDR/kg, and a cost of input of 1,970,414 IDR/ha. The damage assessment methods were validated by comparing the calculated results of damage during past flood events using reported data. The details on the validation of household damage, including the calculation conditions, can be found in Shrestha et al. [32] and that of rice-crop damage in Shrestha et al. [39].

To evaluate the effectiveness of flood control measures, first flood damage to buildings, contents, and rice crops was calculated without considering any flood control measures for flood events of different return periods, i.e., 5-, 10-, 25-, 50-, 100-, 150-, and 200-year floods. Then, flood damage was assessed using different flood control measures to evaluate the effectiveness of each flood control measure for flood risk reduction. By using the calculated results of flood events of different return periods, expected annual damage (EAD) with or without flood control measures was calculated by integrating flood damage for all flood probabilities, using Equation (3) [40].

$$EAD = \frac{1}{2}\sum_{i=1}^{n}\left(\frac{1}{RP_i} - \frac{1}{RP_{i+1}}\right)(D_i + D_{i+1}) \quad (3)$$

where n is the number of return periods considered for damage calculations, RP is the return period, and D is the calculated damage cost.

This study evaluated flood damage reduction by (i) the use of the Wonogiri dam for flood control using its current capacity and (ii) river channel improvements to increase the channel's transport capacity. To evaluate the effectiveness of the flood control dam, this study considered the current flood control operation rules (FCOR) of the dam. Based on the current FCOR, when the inflow into the reservoir exceeds 400 m^3/s, the discharge release from the dam should be kept at 400 m^3/s until the reservoir water level reaches the design flood water level. The effectiveness of damage reduction by the use of the Wonogiri

dam was evaluated by setting a discharge control rate based on FCOR in the river flow simulation. The discharge release from the dam was maintained to be 400 m^3/s when the inflow into the reservoir exceeded 400 m^3/s until the water storage volume reached the maximum flood storage capacity (220×10^6 m^3). When the inflow into the reservoir was below 400 m^3/s or when the dam water storage reached the flood storage capacity, the dam's outflow rate was set to be the same as the inflow rate.

River channel improvements, such as channel widening and deepening (dredging), can increase its capacity to transport water, allowing it to carry a higher flow rate and store a larger volume of water, helping prevent flooding, and potentially reducing flood risk in certain areas. To evaluate the effectiveness of channel improvements for flood control, channel widening or deepening along the river reach, as shown in Figure 4, was considered based on flood inundation analysis. The river channel width or depth was increased by 5% or 10% of the original river width or depth, which was calculated using Equation (1) or Equation (2). Then, flood simulation was conducted with the scenarios of channel widening or deepening. The construction of embankment can be low cost if it uses local materials, lightweight materials, and construction methods that reduce labor and materials and also no resettling of people living at riverbanks is required. Therefore, for our better understanding, flood damage reduction by building embankments along the selected river reach was also evaluated. The quantitative evaluation of flood damage reduction by channel widening or deepening or building embankment provides scientific information for choosing better options for reducing flood damage depending on availability of local resources and materials. In addition, the combined effectiveness of use of existing Wonogiri dam for flood control with channel widening or deepening or building embankment was also evaluated quantitatively.

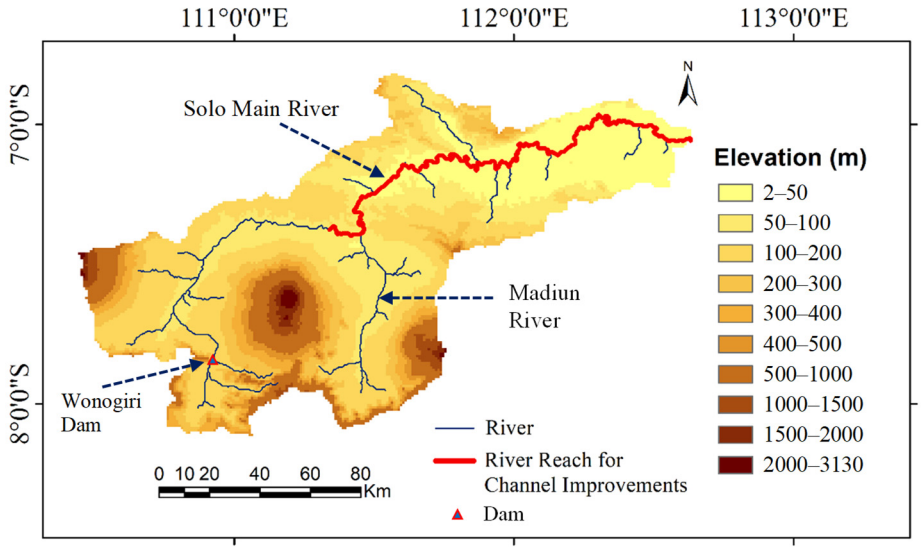

Figure 4. River reach considered (red line) for river channel improvements in the analysis.

3. Results

3.1. Delineation of Flood-Prone Areas and Flood Hazard Analysis

The calibrated and validated WEB-RRI model parameters for the same basin by Shrestha et al. [32] were used in this study. Figure 5 shows the comparison between calculated discharges and observed discharges at the Cepu station for the flood events of calibration and validation [32], and the calculated results agree well with the observations with high Nash–Sutcliffe efficiency (NSE) and r-squared values. The calculated flood inundation area with a flood depth greater than 0.3 m varies from 219.5 km^2 to 1634.3 km^2 for 5-year to 200-year floods under the natural flow condition. Figure 6 shows the calculated

flood inundation depth and extent for a 10-year flood (low-scale flood), 50-year flood (high-scale flood), and 100-year flood (extreme flood). In the cases of high-scale and extreme floods, inundation with high flood depths covers a large area located in the lower reach of the basin and an area upstream of the confluence of the Madiun River (red circle areas). Figure 7 shows the flood inundation probability from high frequency (frequently inundated areas) to low frequency (rarely inundated areas), which was prepared by overlaying inundated areas calculated for different return periods (i.e., 5-, 10-, 25-, 50-, 100-, 150-, and 200-year flood). The results of flood inundation probability are useful for flood zoning that limits development activities in areas of high flood risk.

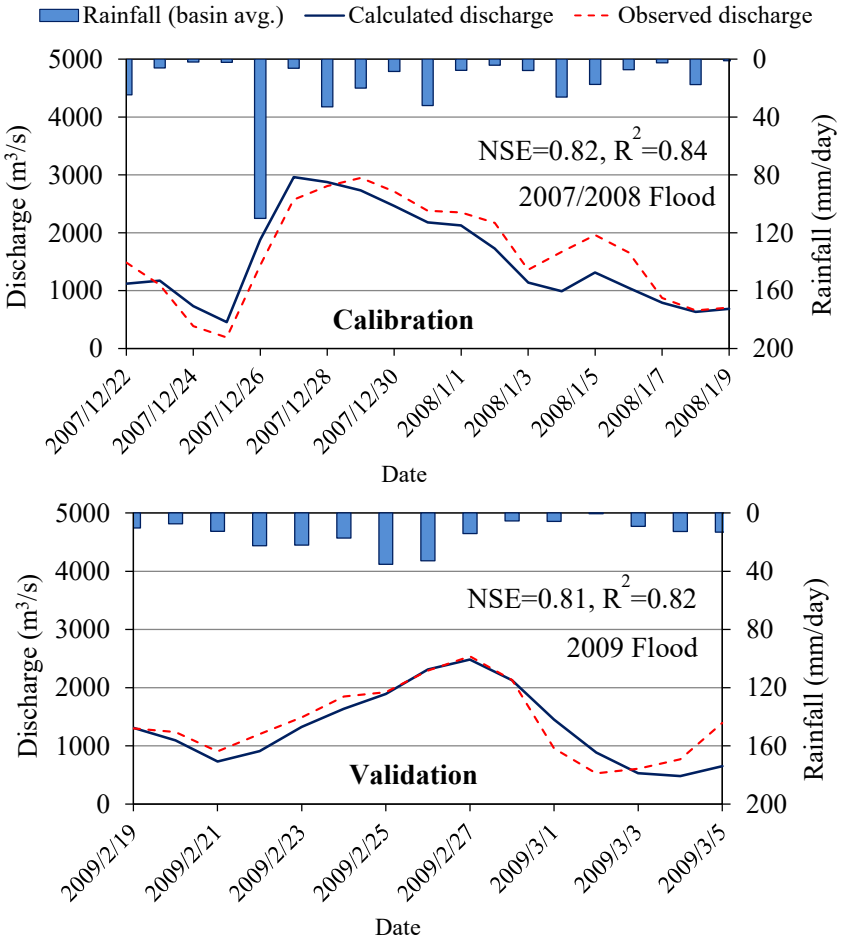

Figure 5. Time-series plots of calculated and observed daily discharges at Cepu station for flood events in 2007/2008 and 2009.

3.2. Flood Exposure Assessment

Figure 8 shows the land cover maps for 1990, 2006, and 2020. Large paddy-field areas (PFA) lie in the low-land areas of the lower basin, where flooding occurs frequently. Table 1 shows the area of each land cover class and its increases or decreases between 1990 and 2006, between 2006 and 2020, and between 1990 and 2020. The rate of changes in LULC was higher in 2006–2020 than in 1990–2006. Plantation forest (PF), settlement and built-up area (SBA), dryland agriculture (DLA), and PFA significantly changed during the period from 1990 to 2020. The study basin was largely dominated by PFA (38.8% of the total area) and PF (23.5% of the total area) in 1990. The PFA decreased from 6155.92 km^2 in 1990 to 5687.02 km^2 in 2020, and PF from 3733.79 km^2 to 3413.91 km^2, while SBA significantly increased from 1714.67 km^2 in 1990 to 2518.34 km^2 in 2020.

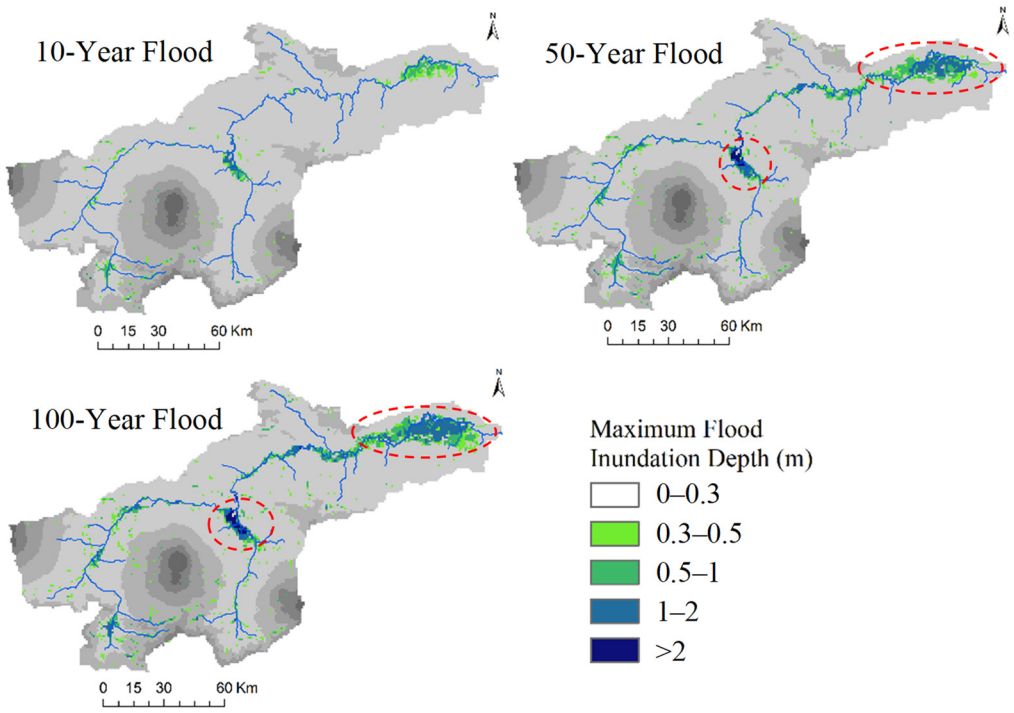

Figure 6. Calculated flood inundation depth and extent areas for 10-, 50-, and 100-year floods.

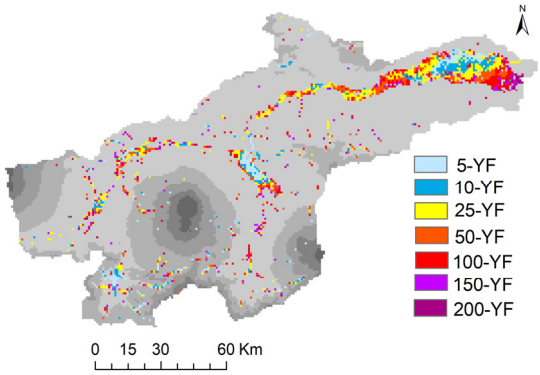

Figure 7. Flood inundation probability from high frequency to low frequency.

Figure 9 shows the loss and gain in the area of LULC during two periods: 1990–2006 and 2006–2020. In the period between 1990 and 2006, the loss areas of PFA were mainly converted to PF and SBA, whereas the gain areas in PFA were mainly from the PF. The loss areas of PF were converted to PFA, DLA, and mixed dryland and shrub (MDS), whereas the gain areas were from DLA, PFA, MDS, secondary dryland forest (SDF), and shrubland (SL). The gain areas of SBA were largely from PFA, MDS, and DLA. In the period between 2006 and 2020, large areas of PFA and PF were converted to other LULCs. The loss areas of PFA in this period were mainly converted to SBA, whereas the gain areas were from MDS, DLA, and SBA. The loss areas of PF were mainly converted to DLA, MDS, and PFA, whereas the gain areas in PF were mainly from MDS. The gain areas of SBA were mainly from PFA, MDS, and DLA. The net changes (increase or decrease) in PF during three periods, 1990–2006, 2006–2020, and 1990–2020, were 164.81, (−) 484.69, and (−) 319.88 km^2, respectively ("−" means decrease in area). They were about (−) 57.18., (−) 411.72, and (−) 468.9 km^2 in the case of PFA. The net increased area in SBA was 83.83 km^2 from 1990 to 2006, 719.84 km^2 from 2006 to 2020, and 803.67 km^2 from 2006 to 2020.

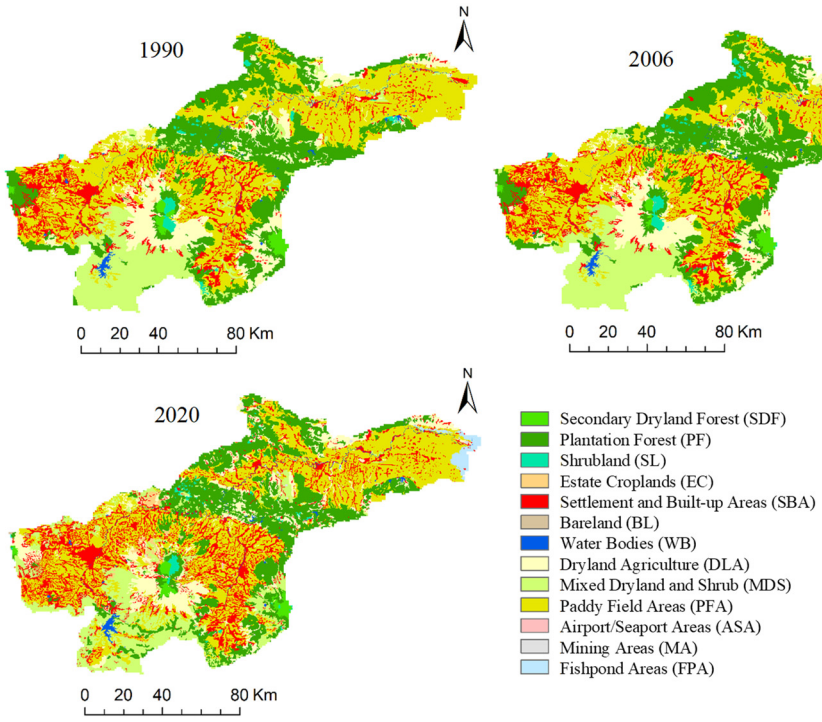

Figure 8. Land cover maps for past years (source: Ministry of Environment and Forestry, Indonesia).

Table 1. Area of each land cover class and changes in area (note: the FPA was not observed in the 1990 and 2006 LULC maps, and the MA was also not observed for 1990).

LULC Type	Area (km^2)			Change in Area (km^2)		
	1990	2006	2020	1990−2006	2006−2020	1990−2020
SDF	170.02	129.86	146.90	−40.16	17.04	−23.12
PF	3733.79	3898.60	3413.91	164.81	−484.69	−319.88
SL	154.76	152.52	106.03	−2.24	−46.49	−48.73
EC	50.70	50.70	116.87	0.00	66.17	66.17
SBA	1714.67	1798.50	2518.34	83.83	719.84	803.67
BL	0.69	21.40	7.76	20.71	−13.64	7.07
WB	121.48	112.41	130.40	−9.07	17.99	8.92
DLA	1811.94	1713.34	1568.31	−98.60	−145.03	−243.63
MDS	1922.58	1860.09	1954.44	−62.49	94.35	31.86
PFA	6155.92	6098.74	5687.02	−57.18	−411.72	−468.9
ASA	2.501	2.50	4.40	0.00	1.90	1.899
MA	-	0.37	19.60	-	19.23	-
FPA	-	-	165.02	-	-	-

Figure 10 shows the calculated flood-exposed area of the LULC class for different flood scales (10-, 50-, and 100-year floods), using the 1990, 2006, and 2020 land cover maps. PFA is highly vulnerable to floods. The calculated flood-exposed PFA for 10-, 50-, and 100-year floods is more than 250, 700, and 950 km^2, respectively. The flood exposure of PFA in the cases of 50- and 100-year floods slightly decreases because of the conversion of PFA to other land cover classes, such as SBA. On the other hand, the flood exposure of SBA increases. The calculated flood-exposed area of SBA for a 100-year flood using the 1990, 2006, and 2020 land cover maps were 129.03, 137.99, and 212.58 km^2, respectively,

indicating a rapid expansion of SBA in the flood-prone areas. In the study basin, the areas of MDS, DLA, and PF were found to be exposed to flooding. The calculated flood-exposed areas of MDS, DLA, and PF for a 100-year flood using the 1990 land cover map were 142.24, 49.27, and 49.12 km^2, respectively, while they were about 65.72, 53.95, and 43.94 km^2, using the 2020 land cover map.

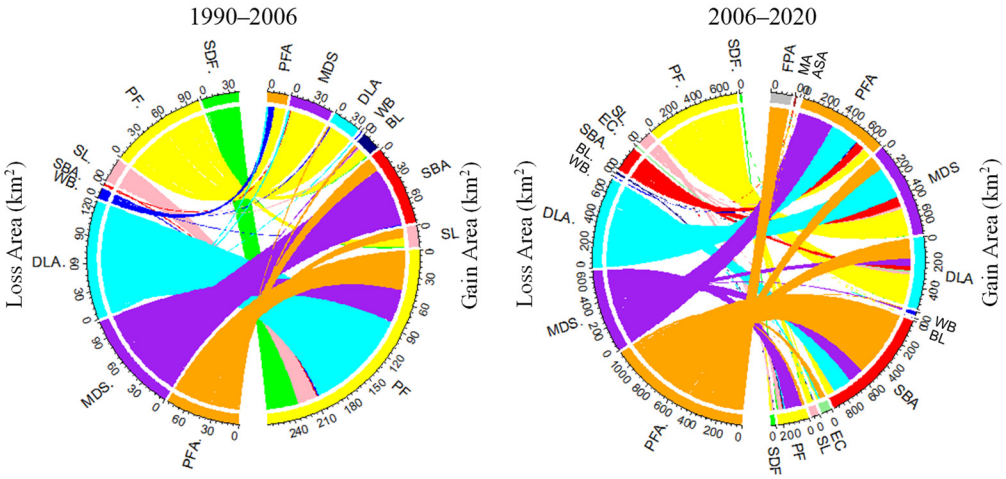

Figure 9. Loss and gain areas of each land cover class during 1990–2006 and 2006–2020 (plotted using circlize–Circular Visualization R-package by Gu et al. [41]).

Figure 11 shows the population distributions in the study area for 2000, 2010, and 2020, based on WorldPop data. The estimated population over the study area in 2000, 2010, and 2020 was 11.71, 11.94, and 12.24 million. The population mainly increased in Surakarta City and the districts located in the low-land areas. Figure 12 shows dynamic changes in basin population and flood-exposed population in the flood-prone areas. Both cases show an increasing trend. The flood-exposed population is increasing due to demographic changes.

3.3. Evaluation of Flood Control Measures for Damage Reduction

To evaluate the effectiveness of flood control measures for flood damage reduction, household and rice-crop damage by different return period floods was calculated based on the 2020 population data and the 2020 PFA data, respectively. Figures 13 and 14 show the spatial distributions of calculated flood damage to household buildings and contents and rice crops, respectively, for 10-, 50-, and 100-year floods without flood control measures. The estimated number of houses for 10-, 50-, and 100-year floods was 45,970, 190,015, and 247,030, respectively. The calculated values of flood damage to buildings and contents for a 10-year flood were IDR 222.1 billion and IDR 198.2 billion, respectively, while they were IDR 1057.1 billion and IDR 940.3 billion for a 50-year flood and IDR 1616.9 billion and IDR 1407.04 billion for a 100-year flood. The increase in the value of both building and content damage between 10- and 50-year floods is more than 370%. The value increase in building and contents damage between 50- and 100-year floods is approximately 50%. The flooded paddy area and the calculated value of rice-crop damage for a 10-year flood were 18,479 ha and IDR 7.68 billion, respectively, while they were about 62,813 ha and IDR 78.48 billion for a 50-year flood and 79,342 ha and IDR 138.13 billion for a 100-year flood. The value increase in rice-crop damage between 10- and 50-year floods is 921% and approximately 76% between 50- and 100-year floods. The results show that the flood damage to households and agricultural crops in the case of a small-scale flood mainly occurred in the low-land areas of the lower basin and the areas immediately upstream of the Madiun River confluence point. However, in the case of high-scale and extreme floods,

flood damage occurred along the Solo River, and the flood damage was severe in areas in the lower basin and immediately upstream of the confluence point.

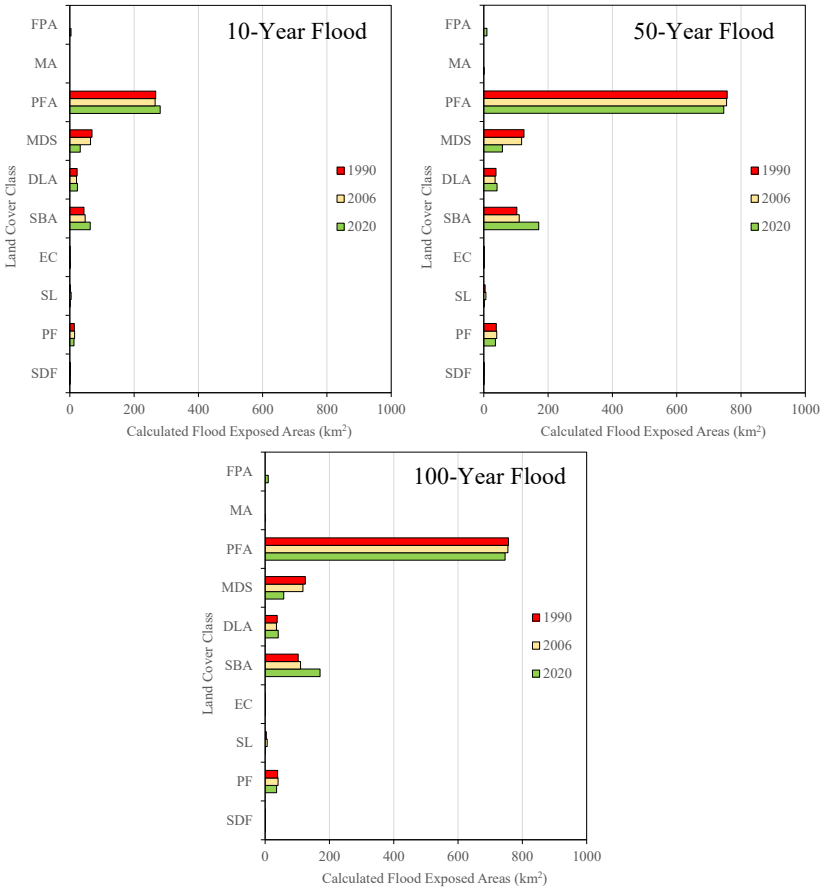

Figure 10. Calculated flood exposed areas of each land cover class in the cases of 10-, 50- and 100-year floods.

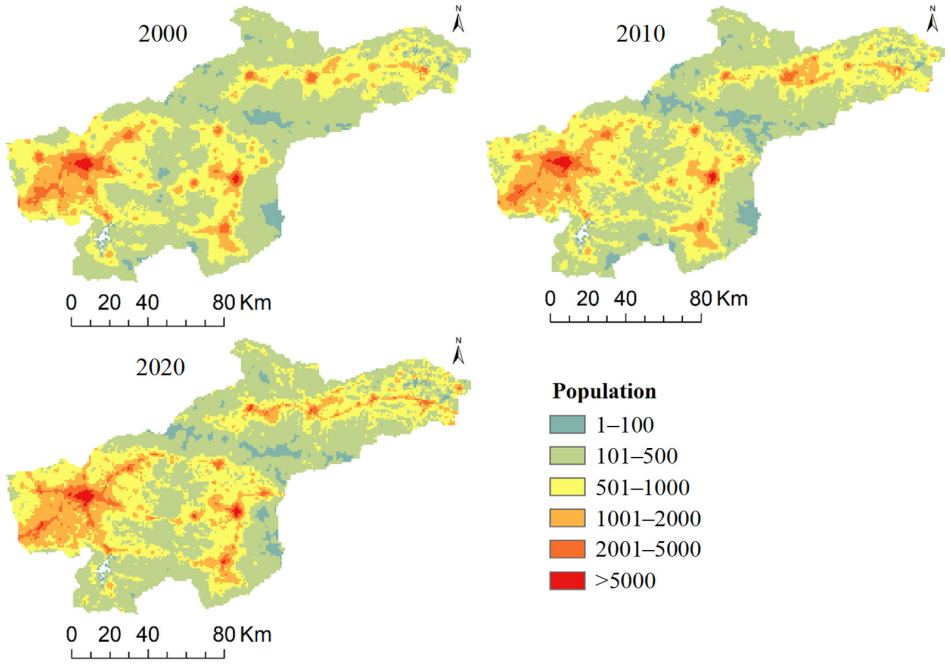

Figure 11. Spatial distribution of population over the basin based on WorldPop Population for 2000, 2010, and 2020.

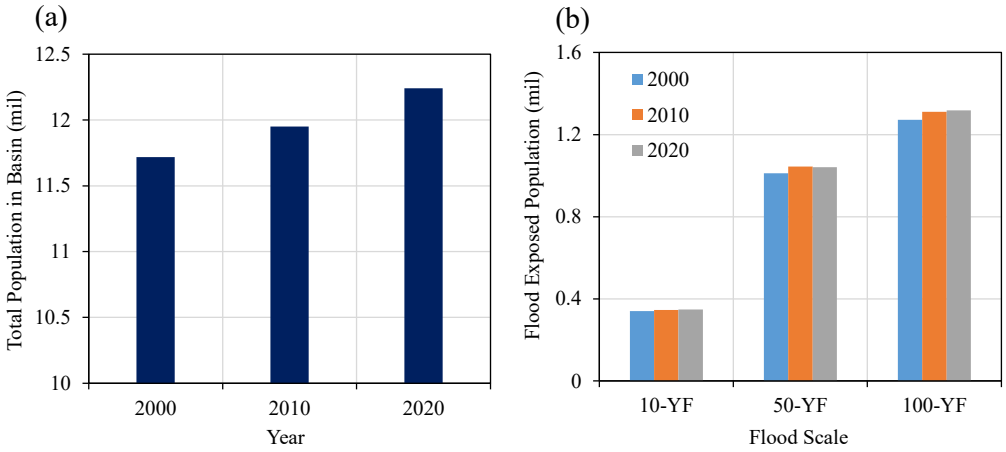

Figure 12. (**a**) Total estimated population in the study area for 2000, 2010, and 2020; and (**b**) calculated flood exposed population using different years' population data (2000, 2010, and 2020) for 10-, 50-, and 100-year flood event cases.

Figure 15 compares the calculated inflow discharge into reservoir and outflow discharge from the dam reservoir with a discharge control rate based on FCOR in the river flow simulation for 10-, 50-, and 100-year floods. The estimated peak inflow discharge into reservoir for 10-, 50-, and 100-year floods was 850, 1003, and 1068 m^3/s, respectively, which was comparatively higher than the set discharge control rate 400 m^3/s. According to the study by JICA [42], the reservoir of Wonogiri dam in the basin often experienced inflow of large-scale flood with peak discharge exceeded 1000 m^3/s. The largest inflow flood peak discharge in 1988 was recorded at 2880 m^3/s, which was more than two times higher than the calculated peak inflow discharge into reservoir for 100-year flood presented in Figure 15. The results clearly indicate that the operation of Wonogiri dam based on current FCOR and available flood storage reservoir capacity can effectively control the inflow flood volume and peak discharge, even during a 100-year flood event.

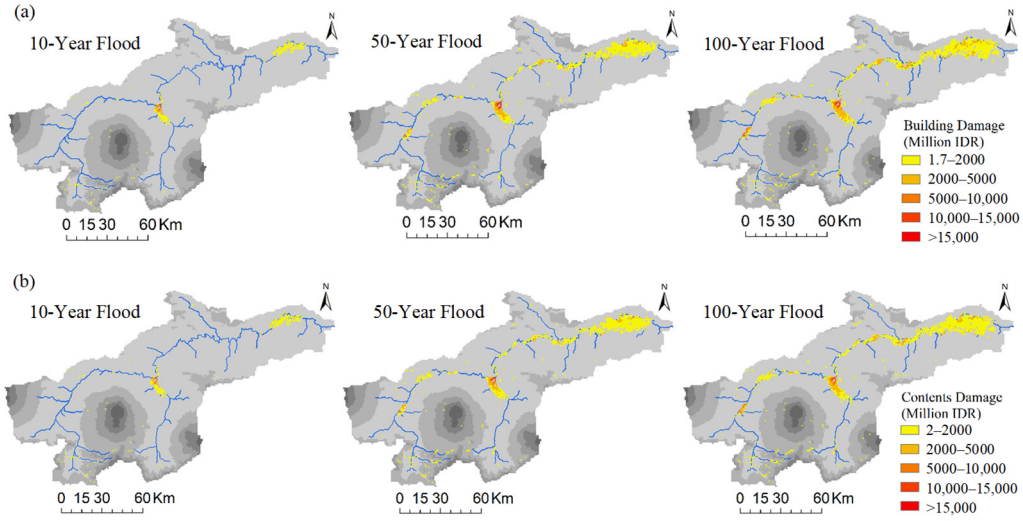

Figure 13. Calculated flood damage to buildings and contents for 10-, 50-, and 100-year floods, without any flood control measures: (**a**) building damage and (**b**) content damage.

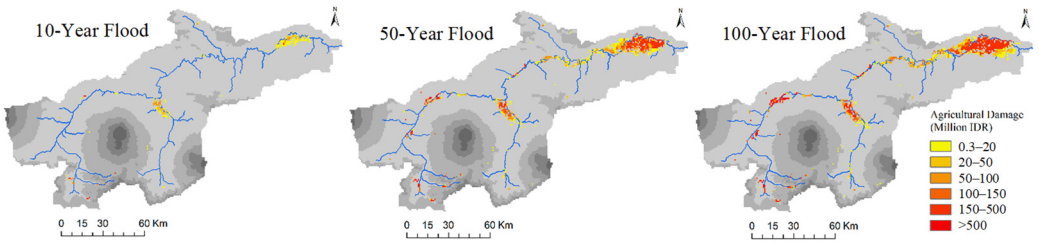

Figure 14. Calculated flood damage to agricultural crops (rice crops) for 10-, 50-, and 100-year floods, without any flood control measures.

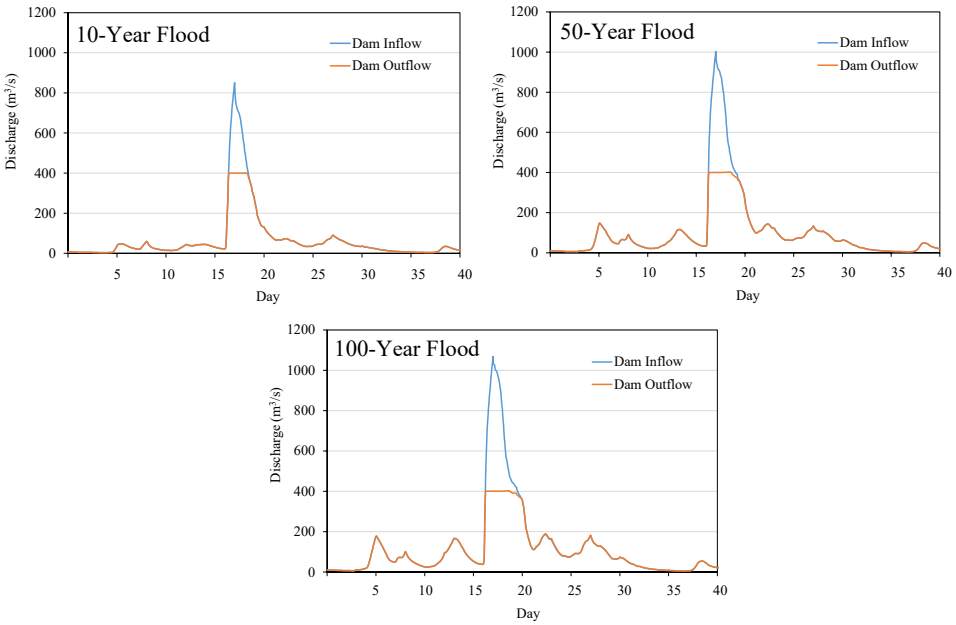

Figure 15. Calculated inflow discharge into reservoir and outflow discharge from the dam for 10-, 50-, and 100-year flood cases.

Figure 16 shows the calculated EAD for household buildings and contents and agricultural crops with and without the use of the Wonogiri dam for flood control. EAD was calculated using the calculated damage cost for different return period floods, i.e., 5-, 10-, 25-, 50-, 100-, 150-, and 200-year floods. The results show that the percentages of EAD reduction in flood damage to residential buildings and contents by discharge control at the Wonogiri dam are 21.2% and 20.9%, respectively. The EAD reduction in rice-crop damage by using the Wonogiri dam for flood control is 25.1%. Even though the Wonogiri dam is located in the upper part of the basin, the use of this dam for flood control based on the current FCOR can reduce EAD by more than 20%.

Figure 17 shows the calculated EAD of building damage, content damage, and rice-crop damage with and without different options of river channel improvement for damage reduction. The figure also shows the EAD reduction by each river channel improvement option. The EAD of building damage decreases by 17–31% through 5–10% river channel deepening compared with the EAD of building damage without river channel improvement, and approximately 10–20% by 5–10% river channel widening. The reduction in the EAD of contents damage by 5–10% river channel deepening or widening is 16–30% or 10–19%. Similarly, the reduction in the EAD of rice-crop damage by 5–10% river channel deepening or widening is 15–28% or 13–17%. The construction of 3-m-high levees can reduce the EAD of building, contents, and rice-crop damage by 40%, 40%, and 37%, respectively.

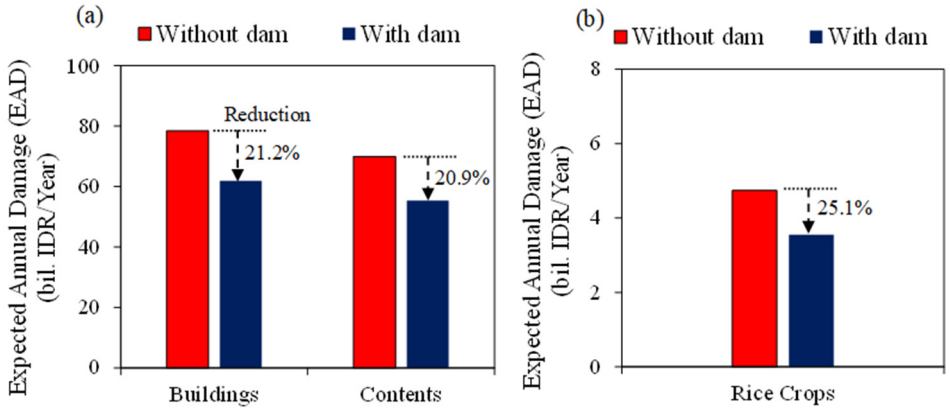

Figure 16. Calculated expected annual damage (EAD) of building, content, and rice-crop damages, with and without dam control function and percentage reduction in EAD by the use of dam for flood control: (**a**) buildings and contents and (**b**) rice crops.

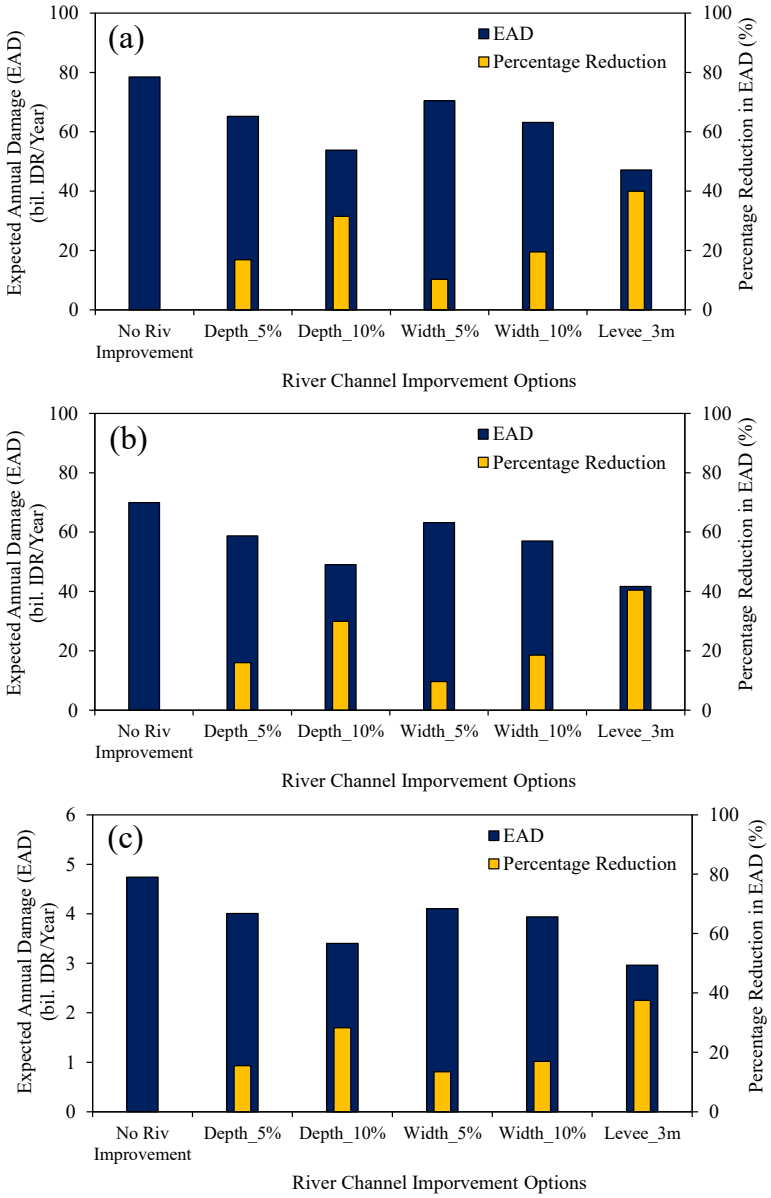

Figure 17. Calculated expected annual damage with and without river channel-improvement options and percentage reduction in EAD by the river channel-improvement options: (**a**) building-damage case, (**b**) content-damage case, and (**c**) rice crop-damage case. (Note: Riv in the figures means River).

The above-discussed results are based on the evaluation of individual effectiveness of the Wonogiri dam or each river channel improvement option for flood control. However, a combination of flood control dam (Wonogiri dam) and river channel improvement works can further reduce the damage or loss. Figure 18 shows calculated results of buildings, contents, and rice-crop damage and reduction of damage by combining the use of the Wonogiri dam for flood control with various river channel improvement options, in the case of 100-year flood. The results show that the flood damage can be reduced by more than 60% by implementing combined flood control option C5 (i.e., *Dam + Levee_3m*), C6 (i.e., *Dam + Depth_5% + Width_5%, + Levee_3m*), or C7 (i.e., *Dam + Depth_10% + Width_10%, + Levee_3m*). The reduction in damage by other combined flood control options, such as C1 (*Dam + Depth_5%*), C2 (*Dam + Depth_10%*) or C3 (*Dam + Width_5%*), or C4 (*Dam + Width_10%*) ranges from 28 to 42% of building damage, from 28 to 41% of content damage, and from 37 to 43% of rice-crop damage.

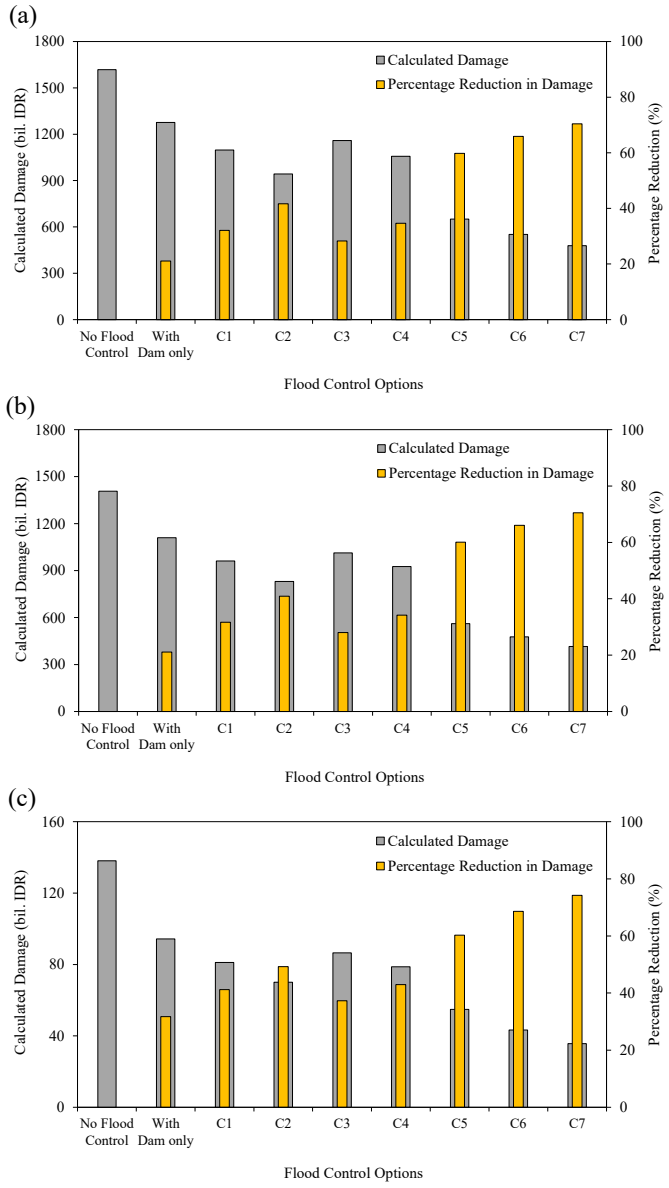

Figure 18. Calculated flood damage in the cases of combination of flood control dam with river channel improvement options for 100-year flood: (**a**) buildings damage, (**b**) contents damage, and (**c**) rice-crop damage (C1, *Dam + Depth_5%*; C2, *Dam + Depth_10%*; C3, *Dam + Width_5%*; C4, *Dam + Width_10%*; C5, *Dam + Levee_3m*; C6, *Dam + Depth_5% + Width_5% + Levee_3m*; and C7, *Dam + Depth_10% + Width_10% + Levee_3m*).

4. Discussion

4.1. Dynamic Changes in Flood Exposure

This study presented the dynamic changes in flood exposures and quantitative evidence on how low-cost flood control measures, such as the use of existing structures like dams and river channel improvements, can effectively reduce flood damage. Large PFAs and SBAs are exposed to flooding in the study area, posing a greater impact on agricultural production and residential areas. Urbanization and development activities are rapidly increasing in the flood-prone areas of the study basin. Flood-exposed population is also increasing in the study area due to demographic changes in flood-prone areas. Swain et al. [43] reported that the key factors for the increased flood-exposure population in the United States are climate change and population growth. Population growth in flood-prone areas puts more people at risk of flooding. Climate change is expected to increase rainfall intensity and flood risk in the study area [39], which may further increase flood exposure. Effective preventive measures are thus necessary to mitigate flood risk in areas with growing populations and development activities.

4.2. Flood Damage Assessment and Quantitative Evaluation of Flood Control Measures

The estimated EAD of residential households (both house and contents damage) without flood control measure for BSRB was IDR 148.38 billion per year (USD 9.1 million per year). In the case of rice-crop damage, it is approximately IDR 4.74 billion per year (USD 0.29 million per year). Shrestha and Kawasaki [28] estimated EAD value of household damage for Bago River basin in Myanmar at MMK 69.8 billion per year (USD 33.2 million per year), and at MMK 5.8 billion per year (USD 2.7 million per year) in the case of rice-crop damage. Budiyono et al. [44] estimated total EAD for Jakarta in Indonesia at USD 333 million per year. Yamamoto et al. [45] estimated the EAD value of direct flood damage to general properties and agriculture in the late 20th century for Japan at JPY 3259 billion per year (USD 21,162 million per year). The estimated EAD values significantly differ between locations due to the varying levels of flood exposure and their exposed value at risk, depending on the location and size of the study area.

To reduce the flood damage, the construction of new flood preventive structural measures might be challenging due to various social, political, and financial issues. However, if existing structures are effectively used by maximizing their current capacity for flood control, flood damage can be reduced without building additional structures. Our findings show that the use of the Wonogiri dam with its current storage capacity can reduce flood damage to the residential and agricultural sectors by more than 20%. Flood damage can be further reduced by releasing reservoir water before a flood starts. The pre-releasing of reservoir water can increase the flood storage capacity, thus further improving flood damage prevention [46], which can be performed using rainfall forecasts [47]. In addition to using existing dams for flood control, river channel improvements have also been practiced in many developing countries to prevent flooding by increasing the river channel capacity. River channel improvements can help control flooding by stabilizing a river channel. The findings also indicated that river channel improvements (e.g., deepening or dredging, widening, and levee construction) aimed at increasing the channel capacity to transport more floodwaters can also reduce flood impact and damage. A recent study by Syaifurahman et al. [48] for the upper part of the BSRB reported that the existing channel cannot accommodate extreme flood discharges and pointed out the importance of channel deepening and widening to reduce flood damage in the study area. The findings of this study show that the reduction in EAD by levee construction is higher than the channel deepening or widening, but investment costs may vary depending on selection of construction materials and methods. In addition, if houses are on riverbanks, extra investment will be

necessary to relocate residents. River channel dredging can be implemented with less effort than the construction of embankments and channel widening, as dredged sediments are usually deposited on riverbanks, particularly in developing countries. However, dredging may need to be performed annually.

River channel widening or deepening increases the flow area, which results in a decrease in the flow speed for the same flow rate. Meanwhile, in the case of levee construction, the flow speed remains unchanged up to the bank stage, but it increases when the river overflows its bank stage. When river water flows higher than the bankfull discharge, the flow area is reduced due to the existence of levee, which leads to an increase in the flow speed. If river channel-improvement works are implemented only in the middle reach of a river, they may increase flood risk in areas downstream of the new structures. To overcome this issue, river channel-improvement works should be carried out continuously from the middle to lower reaches or only in the lower reaches [30].

The use of Wonogiri dam and the river channel-improvement works for flood control in the study area can significantly reduce the flood damage to buildings, household contents, and agricultural crops. In addition, nature-based solutions like floodplain restoration, use of retention ponds, and the use of wetlands for flood regulation can also reduce the flood risk, which are more eco-friendly flood defenses than structural measures and also enhance biodiversity. However, these solutions may require replanting trees, creating retention ponds and wetlands, and preserving natural floodplains; and also, they may not be effective for large-scale flooding. Moreover, elevating and floodproofing solutions by households living in the flood-prone areas (e.g., elevating the building by raising the plinth level, building new houses on elevated ground above the flood level, building houses with flood resistance materials, and building barrier walls) are also other possible feasible options for reducing the flood impact [49,50]. In the case of agricultural damage reduction, establishment of adequate drainage capacity, the use of submergence-tolerant rice varieties in flood-prone areas during the monsoon season, and changing the cropping pattern or schedule to avoid the flood can also help in reducing the crop loss [51].

Increasing flood exposure due to demographic changes has significant social and economic implications, including widespread physical property damage, agricultural crop damage, and disruption to daily life, while flood control measures presented in this study can reduce these impacts by protecting properties, reducing economic losses, and enhancing community resilience. The implementation of effective flood control measures can not only reduce flood damage but also contribute to the long-term improvement of livelihoods and hereafter the socioeconomic development in the flood-prone areas, allowing for more stable economic activity and improved quality of life [52]. The flood control options presented in this study for the BSRB can significantly impact local communities by reducing flood damage, which will contribute to improving the living conditions of people living in the flood-prone areas. However, when implementing river channel improvements, particularly constructing embankment, displacement or relocation of houses located along the river might be required.

4.3. Long-Term Strategies for Reducing Flood Risk

Quantifying exposed people in flood-prone areas spatiotemporally and evaluating the effectiveness of flood control measures provide scientific information that can be useful for preparing, planning, and implementing flood preventive measures and reducing property and human risks. The quantitative results of flood exposure and damage can be used to build a resilient society and also to help policy- and decision-makers establish flood adaptation measures and policies required for risk reduction, such as land use regulations, guidelines for building constructions, and restrictions on development activities

in flood-prone areas [49]. A comprehensive flood management strategy combining both structural measures (like those presented in this study) with non-structural approaches, like hazard and risk mapping, land use planning, urban-planning regulations, and resilient infrastructure investments, is crucial for long-term flood mitigation.

Land use planning, such as land use restrictions in flood-prone areas through land use zoning with building restrictions also plays a key role in reducing damage by extreme flood events. Relocating existing buildings from flood-prone areas can be expensive, but restrictions on constructing new buildings in flood-prone areas anticipating high flood depths can help reduce damage [49]. Flood damage reduction is also possible in paddy fields in flood-prone areas with high flood depths by introducing submergence-tolerant rice varieties, new cropping practices, or different rice-cropping calendars, avoiding flooding and other adverse effects taking place potentially due to climate change. Figure 19 shows a decrease in damage owing to land use restrictions in the study flood-prone areas with high flood depths (2.5, 2.0, and 1.5 m). Flood damage was calculated in the case of applying land use restrictions, relocating existing buildings; adjusting the rice-cropping calendar; or changing cropping practices for the flood-prone areas with high flood depths (≥2.5, 2.0, or 1.5 m), assuming 50- and 100-year floods.

In addition, establishment of policies for urban planning regulations (e.g., zoning restrictions in flood-prone areas, mandatory building elevation requirements in flood-prone areas, regulations on impervious surfaces to reduce runoff, and guidelines for stormwater management systems) and investment in sustainable and resilient infrastructures (e.g., allocating funds or budget for infrastructures designed for reducing the flood impact are also crucial for long-term flood control because they help communities withstand and recover from extreme weather events. Furthermore, mapping flood hazards and risks can also be important and informative non-structural approaches to reducing losses and preventing damage from floods [28].

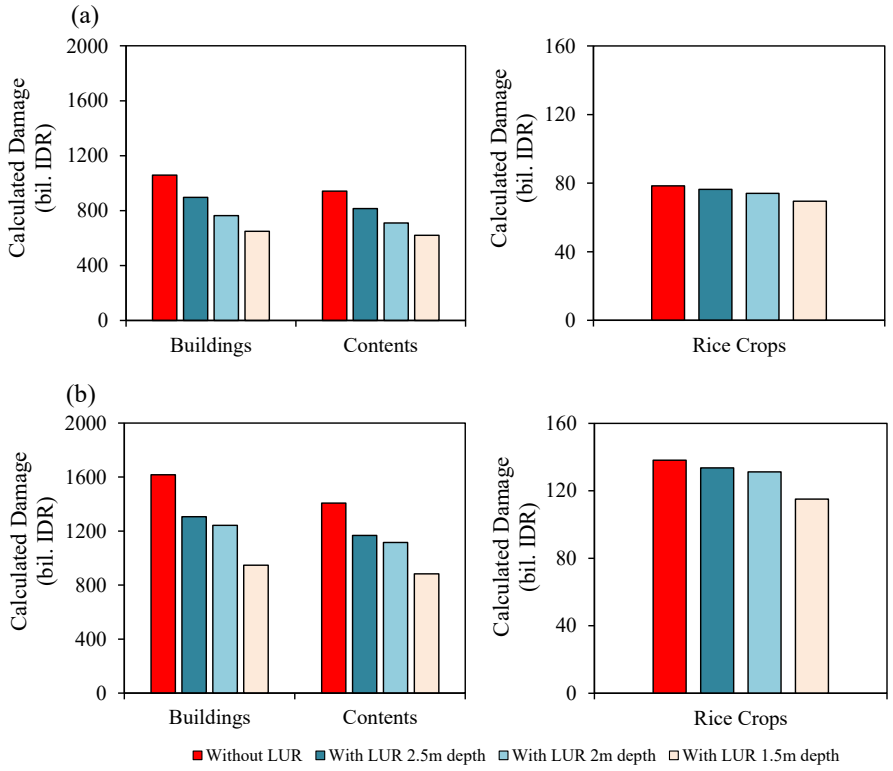

Figure 19. Calculated damage with and without land use restriction (LUR) alone in the flood-prone areas with high flood depth: (**a**) 50-year flood case and (**b**) 100-year flood case.

4.4. Uncertainties and Further Improvements

Flood damage assessment results are often subject to significant uncertainties due to a variety of factors, such as data limitations, quality of topographical data used in the flood hazard prediction, selection of spatial scale in flood modeling, assumptions of data used in damage estimation, variations in exposure characteristics, and the lack of detailed information on characteristics of exposures. This study used average exposed values of buildings, contents, and agricultural crops in assessing the damage, and the use of average exposed values for large areas can also lead to uncertainty in the results; to reduce this uncertainty, it is important to consider a wider range of data from various locations in further studies.

This study used globally available topographical data at 30-arc second spatial resolution, focusing on hazard and risk assessment at basin level. For local community-level evacuation purposes, detailed flood inundation simulation with an even finer spatial resolution can be beneficial. In addition, the reliability of flood inundation results can be further improved by incorporating ground-based topographical data. The river channel geometry was assumed to be rectangular, and its shapes were defined by depth and width. Because the river cross-sectional data can hardly be obtained, this study used regime equations to calculate river depth and width. However, incorporation of river cross-sectional data with the actual geometry shape of a river cross-section in a model simulation can further enhance the reliability of the flood simulation results.

In this study, the number of distributed houses was estimated based on the gridded population counts and the average family size. When estimating the number of houses based on population, uncertainty can arise due to several factors, such as variations in family size, demographic shifts and migrations, and data quality issues in gridded population counts. For example, the number of inundated houses for 100-year flood (without flood control-measures case) using the average family size of 3.7 people was 247,030; however, it varies to 261,146 when using an average family size of 3.5 people and to 234,361 using an average family size of 3.9 people. However, Shrestha et al. [32] validated the estimated number of inundated houses for the 2007/2008 flood event with the reported inundated houses and found estimated inundated houses (162,505) to be reasonably agreeable with the reported inundated house (165,117). The reliability of the flood damage estimation for households can be further improved by incorporating houses data and information available from the local government. In addition, the use of the average value of rice yield, farm gate price of rice, and cost of input to calculate volume and value of rice-crop loss can also lead to uncertainty in the rice crop-damage estimation, as these values vary from place to place, and this uncertainty can be reduced by incorporating a wider range of data from different locations.

This study specifically focused on flood damage to residential buildings and assets, and rice crops. However, it is also recommended to consider flood damage to other sectors, such as roads, bridges, and other types of infrastructure, as well as the risk of human loss. In addition, this study did not take into account the potential future impact of climate change, and in further studies, it will also be crucial to incorporate the impacts of climate change, particularly the projected future climate change in the assessment of the effectiveness of flood control measures and evaluating potential future damage.

5. Conclusions

This study focused on the quantitative analysis of spatiotemporal changes in land cover areas and people exposed to flood risk, and it also aimed to evaluate the effectiveness of the use of an existing dam for flood control and river channel-improvement works for reducing flood damage. This study revealed that the PF, SBA, DLA, and PFA in the study

basin significantly changed during the period of 1990—2020. The areas of PF, DLA, and PFA decreased from 1990 to 2020, whereas the area of SBA increased rapidly. The large paddy fields are at high risk of flooding, indicating a significant impact of flooding on agricultural production; however, the extent of flood impact on agricultural production depends on several factors, such as crop type, growth stage, timing of flooding, and flood characteristics. The findings of this study also indicated that the SBA areas are rapidly expanding in the flood-prone areas. Individual protection measures should be taken if settlements expand into flood-prone areas. The flood-exposed population also relatively increased from 1990 to 2020 in the study areas. The exposure assessment focusing on LULC and population presented in this study enables us to understand spatiotemporal changes in flood exposure, thus helping is plan land use regulations.

The quantitative estimation of flood damage in monetary values with and without flood control options provides scientific information to understand the effectiveness of flood control options in reducing flood damage and also to help policy- and decision-makers implement preventive measures to reduce damage more effectively. The findings show that the increases in rainfall intensity are also one of the key drivers of increased flood damage. The increase in the monetary value of the damage to buildings and contents between 10- and 50-year floods was more than 370% and about 50% between 50- and 100-year floods. The increase in the monetary value of rice-crop damage between 10- and 50-year floods was more than 921%, and it was about 76% between 50- and 100-year floods. The findings show that the use of the Wonogiri dam for flood control can reduce the flood damage in its downstream areas by more than 20%. The results also revealed that the reduction rate in EAD due to levee construction is higher than that due to channel dredging or widening. The results also show that the flood damage can be reduced by more than 60% by implementing a combination of flood control dam with river channel improvements.

The estimation of flood damage with different scenarios of flood control options enables us to better manage flood risk in the future. The results presented in this study can be useful to establish flood control measures and policies required for reducing flood risk, such as land use regulations and guidelines for better preparedness and emergency response activities.

Author Contributions: Conceptualization, B.B.S., M.R. and D.K.; methodology, B.B.S., M.R. and D.K.; validation, B.B.S. and M.R.; formal analysis, B.B.S.; investigation, B.B.S.; data curation, B.B.S.; writing—original draft preparation, B.B.S.; writing—review and editing, B.B.S., M.R. and D.K.; visualization, B.B.S. All authors have read and agreed to the published version of the manuscript.

Funding: This work was conducted by Theme 4 of the Advanced Studies of Climate Change Projection (SENTAN Program), Grant Number JPMXD0722678534, supported by the Ministry of Education, Culture, Sports, Science, and Technology (MEXT), Japan.

Data Availability Statement: The sources data that support the findings of this study are available from the related organizations and the sources mentioned in this article.

Acknowledgments: The authors would like to thank the Research and Development Center for Water Resources (PUSAIR), the Bengawan Solo River Basin Organization (BBWS Bengawan Solo), Ministry of Public Works and Housing, Indonesia, for providing rainfall and discharge data; and the Directorate of Forest Resources Inventory and Monitoring, Directorate General of Forestry Planning and Environmental Administration, Ministry of Environment and Forestry, Indonesia, for providing land cover map data for the study area.

Conflicts of Interest: The authors declare no conflicts of interest.

References

1. Mohamed, S.A.; El-Raey, M.E. Assessment, prediction and future simulation of land cover dynamics using remote sensing and GIS techniques. *Assiut Univ. Bull. Environ. Res.* **2018**, *21*, 37–49.
2. Balogun, I.A.; Ishola, K.A. Projection of future changes in landuse/landcover using multi-layer perceptron Markov model over Akure city, Nigeria. *Glob. J. Sci. Front. Res.* **2017**, *17*, 31–44.
3. Binutha, R.; Somashekar, R.K. Future prediction of land cover in Devikulam Taluk, Kerala. *Int. J. Sci. Nat.* **2014**, *5*, 677–683.
4. Lv, J. Using historical remote sensing image to predict future land use in Panjin city, China. *AIP Conf. Proc.* **2017**, *1864*, 020175. [CrossRef]
5. Shrestha, B.B. Approach for analysis of land-cover changes and their impact on flooding regime. *Quaternary* **2019**, *2*, 27. [CrossRef]
6. Yuliyanto, F.; Prasasti, I.; Pasaribu, J.M.; Fitriana, H.L.; Zylshal; Haryani, N.S.; Sofan, P. The dynamics of land use/land cover change modeling and their implication for the flood damage assessment in the Tondano watershed, North Sulawesi, Indonesia. *Model. Earth Syst. Environ.* **2016**, *2*, 47. [CrossRef]
7. Memarian, H.M.; Balasundram, S.K.; Talib, J.B.; Sung, C.T.B.; Sood, A.M.; Abbaspour, K. Validation of CA-Markov for simulation of land use and cover change in the Langat Basin, Malaysia. *J. Geogr. Inf. Syst.* **2012**, *4*, 542–554. [CrossRef]
8. Hadi, S.J.; Shafri, H.Z.M.; Mahir, M.D. Modeling LULC for the period 2010-2030 using GIS and remote sensing: A case study of Tikrit, Iraq. *IOP Conf. Ser. Earth Environ. Sci.* **2014**, *20*, 012053. [CrossRef]
9. Khawaldah, H.A. A prediction of future land use/land cover in Amman area using GIS-based Markov model and remote sensing. *J. Geogr. Inf. Syst.* **2016**, *8*, 412–427. [CrossRef]
10. Patil, S.D.; Gu, Y.; Dias, F.S.A.; Stieglitz, M.; Turk, G. Predicting the spectral information of future land cover using machine learning. *Int. J. Remote Sens.* **2017**, *38*, 5592–5607. [CrossRef]
11. Khawaldah, H.A.; Farhan, I.; Alzboun, N.M. Simulation and prediction of land use and land cover change using GIS, remote sensing and CA-Markov model. *Glob. J. Environ. Sci. Manag.* **2020**, *6*, 215–232. [CrossRef]
12. Nath, B.; Wang, Z.; Ge, Y.; Islam, K.; Singh, R.P.; Niu, Z. Land use and land cover change modeling and future potential landscape risk assessment using Markov-CA model and analytical Hierarchy process. *Int. J. Geo-Inf.* **2020**, *9*, 134. [CrossRef]
13. Nguyen, H.T.T.; Plam, T.A.; Doan, M.T.; Tran, P.T.X. Land use/land cover change prediction using multi-temporal satellite imagery and multi-layer perceptron Markov model. *Int. Arch. Photogramm. Remote Sens. Spat. Inf. Sci.* **2020**, *44*, 99–105. [CrossRef]
14. Ruben, G.B.; Zhang, K.; Dong, Z.; Xia, J. Analysis and projection of land-use/land-cover dynamics through scenario-based simulations using the CA-Markov model: A case study in Guanting reservoir basin, China. *Sustainability* **2020**, *12*, 3747. [CrossRef]
15. Abbas, Z.; Yang, G.; Zhong, Y.; Zhao, Y. Spatiotemporal change analysis and future scenario of LULC using the CA-ANN approach: A case study of the Greater Bay Area, China. *Land* **2021**, *10*, 584. [CrossRef]
16. Ardiansah, T.; Rijal, S.; Barkey, R.A. Land use change projection in Bonehau watershed 2031. *IOP Conf. Ser. Earth Environ. Sci.* **2021**, *870*, 012028. [CrossRef]
17. El-Hamid, H.T.A.; Kaloop, M.R.; Abdalla, E.M.; Hu, J.W.; Zarzoura, F. Assessment and prediction of land-use/land-cover change around Blue Nile and White Nile due to flood hazards in Khartoum, Sudan, based on geospatial analysis. *Geomat. Nat. Hazards Risk* **2021**, *12*, 1258–1286. [CrossRef]
18. Leta, M.K.; Demissie, T.A.; Tränckner, J. Modeling and prediction of land use land cover change dynamics based on land change modeler (LCM) in Nashe watershed, upper Blue Nile basin, Ethiopia. *Sustainability* **2021**, *13*, 3740. [CrossRef]
19. Tadese, S.; Soromessa, T.; Bekele, T. Analysis of the current and future prediction of land use/land cover change using remote sensing and the CA-Markov model in Majang Forest Biosphere Reserves of Gambella, Southwestern Ethiopia. *Sci. World J.* **2021**, *2021*, 6685045. [CrossRef] [PubMed]
20. Azari, M.; Billa, L.; Chan, A. Multi-temporal analysis of past and future land cover change in the highly urbanized state of Selangor, Malaysia. *Ecol. Process* **2022**, *11*, 2. [CrossRef]
21. Baig, M.F.; Mustafa, M.R.U.; Baig, I.; Takaijudin, H.B.; Zeshan, M.T. Assessment of land use land cover changes and future predictions using CA-ANN simulation for Selangor, Malaysia. *Water* **2022**, *14*, 402. [CrossRef]
22. Cruz, J.d.S.; Blanco, C.J.C.; Júnior, J.F.d.O. Modeling of land use and land cover change dynamics for future projection of the Amazon number curve. *Sci. Total Environ.* **2022**, *811*, 152348. [CrossRef] [PubMed]
23. Muhammad, R.; Zhang, W.; Abbas, Z.; Guo, F.; Gwiazdzinski, L. Spatiotemporal change analysis and prediction of future land use and land cover changes using QGIS MOLUSCE plugin and remote sensing big data: A case study of Linyi, China. *Land* **2022**, *11*, 419. [CrossRef]
24. Bouwer, L.M.; Jonkman, S.N. Global mortality from storm surges is decreasing. *Environ. Res. Lett.* **2018**, *13*, 014008. [CrossRef]
25. Smith, A.; Bates, P.D.; Wing, O.; Sampson, C.; Quinn, N.; Neal, J. New estimates of flood exposure in developing countries using high-resolution population data. *Nat. Commun.* **2019**, *10*, 1814. [CrossRef]
26. Mohanty, M.P.; Simonovic, S.P. Changes in floodplain regimes over Canada due to climate change impacts: Observations from CMIP6 models. *Sci. Total Environ.* **2021**, *792*, 148323. [CrossRef] [PubMed]

27. Tate, E.; Rahman, M.A.; Emrich, C.T.; Sampson, C.C. Flood exposure and social vulnerability in the United States. *Nat. Hazards* **2021**, *106*, 435–457. [CrossRef]
28. Shrestha, B.B.; Kawasaki, A. Quantitative assessment of flood risk with evaluation of the effectiveness of dam operation for flood control: A case of the Bago River Basin of Myanmar. *Int. J. Disaster Risk Reduct.* **2020**, *50*, 101707. [CrossRef]
29. Kawasaki, A.; Kawamura, G.; Zin, W.W. A local level relationship between floods and poverty: A case in Myanmar. *Int. J. Disaster Risk Reduct.* **2020**, *42*, 101348. [CrossRef]
30. IDI (Infrastructure Development Institute—Japan). *The River Law with Commentary by Article, Legal Framework for River and Water Management in Japan*; IDI Water Series; IDI: Bunkyō, Japan, 2018; No. 4; Available online: http://www.idi.or.jp/wp/wp-content/uploads/2018/05/RIVERE.pdf (accessed on 27 December 2024).
31. Rasmy, M.; Sayama, T.; Koike, T. Development of water and energy Budget-based Rainfall-Runoff-Inundation model (WEB-RRI) and its verification in the Kalu and Mundeni River Basins, Sri Lanka. *J. Hydrol.* **2019**, *579*, 124163. [CrossRef]
32. Shrestha, B.B.; Rasmy, M.; Shinya, T. Assessment of flood damage to residential houses and analysis of effectiveness of flood damage reduction measures. *J. JSCE Spec. Issue (Hydraul. Eng.)* **2024**, *12*, 23–16158. [CrossRef]
33. Sayama, T.; Ozawa, G.; Kawakami, T.; Nabesaka, S.; Fukami, K. Rainfall-runoff-inundation analysis of the 2010 Pakistan flood in the Kabul River basin. *Hydrol. Sci. J.* **2012**, *57*, 298–312. [CrossRef]
34. Kudo, S.; Sayama, T.; Hasegawa, A.; Iwami, Y. Analysis of flood risk change in future climate in terms of discharge and inundation in the Solo River Basin. In Proceedings of the International Conference on Water Resources and Environment Research (ICWRER), Kyoto, Japan, 5–9 June 2016.
35. Iwami, Y.; Hasegawa, A.; Miyamoto, M.; Kudo, S.; Yamazaki, Y.; Ushiyama, T.; Koike, T. Comparative study on climate change impact on precipitation and floods in Asian river basins. *Hydrol. Res. Lett.* **2016**, *11*, 24–30. [CrossRef]
36. Shrestha, B.B.; Perera, E.D.P.; Kudo, S.; Miyamoto, M.; Yamazaki, Y.; Kuribayashi, D.; Sawano, H.; Sayama, T.; Magome, J.; Hasegawa, A.; et al. Assessing flood disaster impacts in agriculture under climate change in the river basins of Southeast Asia. *Nat. Hazards* **2019**, *97*, 157–192. [CrossRef]
37. Syldon, P.; Shrestha, B.B.; Miyamoto, M.; Tamakawa, K.; Nakamura, S. Assessing the impact of climate change on flood inundation and agriculture in the Himalayan mountainous region of Bhutan. *J. Hydrol. Reg. Stud.* **2024**, *52*, 101687. [CrossRef]
38. Bösmeier, A.S.; Himmelsbach, I.; Seeger, S. Reliability of flood marks and practical relevance for flood hazard assessment in southwestern Germany. *Nat. Hazards Earth Syst. Sci.* **2022**, *22*, 2963–2979. [CrossRef]
39. Shrestha, B.B.; Rasmy, M.; Ushiyama, T.; Acierto, R.A.; Kawamoto, T.; Fujikane, M.; Shinya, T.; Kubota, K. Assessment of future risk of agricultural crop production under climate and social changes scenarios: A case of the Solo River basin in Indonesia. *J. Flood Risk Manag.* **2025**, *18*, e13052. [CrossRef]
40. Olsen, A.S.; Zhou, Q.; Linde, J.J.; Arnbjerg-Nielsen, K. Comparing methods of calculating expected annual damage in urban pluvial flood risk assessments. *Water* **2015**, *7*, 255–270. [CrossRef]
41. Gu, Z.; Gu, L.; Eils, R.; Schlesner, M.; Brors, B. circlize implements and enhances circular visualization in R. *Bioinformatics* **2014**, *30*, 2811–2812. [CrossRef] [PubMed]
42. JICA (Japan International Cooperation Agency). *The Study on Countermeasures for Sedimentation in the Wonogiri Multipurpose Dam Reservoir in the Republic of Indonesia*; JICA: Tokyo, Japan, 2007. Available online: https://openjicareport.jica.go.jp/pdf/11863909_01.pdf (accessed on 6 February 2025).
43. Swain, D.L.; Wing, O.E.J.; Bates, P.D.; Done, J.M.; Johson, K.A.; Cameron, D.R. Increased flood exposure due to climate change and population growth in the United States. *Earth's Future* **2020**, *8*, e2020EF001778. [CrossRef]
44. Budiyono, Y.; Aerts, J.; Brinkman, J.; Marfai, M.A.; Ward, P. Flood risk assessment for delta mega-cities: A case study of Jakarta. *Nat. Hazards* **2015**, *75*, 389–413. [CrossRef]
45. Yamamoto, T.; Kazama, S.; Touge, Y.; Yanagihara, H.; Tada, T.; Yamashita, T.; Takizawa, H. Evaluation of flood damage reduction throughout Japan from adaptation measures taken under a range of emissions mitigation scenarios. *Clim. Change* **2021**, *165*, 2021. [CrossRef]
46. Wei, G.; Liang, G.; Ding, W.; He, B.; Wu, J.; Ren, M.; Zhou, H. Deriving optimal operating rules for flood control considering pre-release based on forecast information. *J. Hydrol.* **2022**, *615*, 128665. [CrossRef]
47. Nakamura, R.; Shimatani, Y. Extreme-flood control operation of dams in Japan. *J. Hydrol. Reg. Stud.* **2021**, *35*, 100821. [CrossRef]
48. Syaifurahman, A.; Nurzain, D.A.; Prastica, R.M.S. River engineering for flooding characteristics in the upper stream part of Bengawan Solo sub-watershed. *IOP Conf. Ser. Earth Environ. Sci.* **2021**, *622*, 012001. [CrossRef]
49. Shrestha, B.B.; Kawasaki, A.; Zin, W.W. Development of flood damage assessment method for residential areas considering various house types for Bago Region of Myanmar. *Int. J. Disaster Risk Reduct.* **2021**, *66*, 102602. [CrossRef]
50. Alabbad, Y.; Yildirim, E.; Demir, I. Flood mitigation data analytics and decision support framework: Iowa Middle Cedar Watershed case study. *Sci. Total Environ.* **2022**, *814*, 152768. [CrossRef] [PubMed]

51. Shrestha, B.B.; Kawasaki, A.; Zin, W.W. Development of flood damage functions for agricultural crops and their applicability in regions of Asia. *J. Hydrol. Reg. Stud.* **2021**, *36*, 100872. [CrossRef]
52. Yamagami, C.; Kawasaki, A. Reevaluating the benefit of flood risk management for flood-prone livelihoods. *Int. J. Disaster Risk Reduct.* **2024**, *106*, 104416. [CrossRef]